Adaptive optics center of excellence for national security

Brij Agrawal
Naval Postgraduate School, 1 University Circle, Monterey, CA, USA 93943

ABSTRACT

This paper provides an overview of research at the Adaptive Optics Center of Excellence for national security (AOCoE) at the Naval Postgraduate School (NPS). The Center was established in 2011 with the sponsorship of the Office of Naval Research, National Reconnaissance Office, and Air Force research Laboratory. Research is in two areas: Segmented Mirror telescope (SMT) for imaging satellites and High Energy Laser Beam Control. SMT consists of a 3 meter diameter telescope with six segments and each segment has actuators for surface control and segment alignment. SMT research areas include developing improved techniques for surface control and segment alignment, and reduction in segment vibration by using tuned mass dampers. Research is also performed in adding a deformable mirror into the SMT optical path to correct for residual beam aberration not corrected by the primary mirror actuators. For high energy laser beam control the research areas are acquisition, tracking, and pointing, optical beam jitter control, and application of adaptive optics for correcting beam aberration due to air turbulence. The current focus is on adaptive optics for deep turbulence.

Keywords: Adaptive Optics

1. INTRODUCTION

Adaptive Optics (AO) is finding applications in several areas, such as space telescopes, ground telescopes, high energy lasers, and laser communications. For space telescopes, adaptive optics is used for correcting the surface of primary mirrors. Other applications primarily use adaptive optics for correcting aberrations in the optical beam due to air turbulence. Adaptive optics is finding applications on several major Department of Defense (DoD) programs. It is a relatively new technology and research, development, and demonstration is required in several areas. An NSF funded center, Center for Adaptive Optics, was established at the University of California Santa Cruz. The focus of the center was mainly on civilian applications. An Adaptive Optics Center of Excellence for National security (AOCoE) was established in May 2011 at the Naval Postgraduate School (NPS) with the sponsorship of the Office of Naval Research, National Reconnaissance Office, and Air Force Research Laboratory. The objectives of the Center are as follows: 1. Conduct research in Adaptive Optics and related technologies focused on national security applications including classified research; 2. Establish and operate the Segmented Mirror Telescope (SMT) and High Energy Beam Control Testbed (HBCT) as a national users facility available to agencies or institutions within the national security community to address specific scientific and technical research questions; 3. Deepen the technical expertise and increase the throughput of NPS military students in AO; 4.Serve as a portal by which new developments in the academic AO community can be migrated to national security missions; and 5. Serve as a magnet for top civilian students to careers in the Department of Defense and the Directorate of National Intelligence. This paper provides an overview of research focus of AOCoE in two major areas, Segmented Mirror Telescope and High Energy Beam Control.

2. SEGMENTED MIRROR TELESCOPE TESTBED

Several future space imaging missions will need larger mirrors, 10-20 m diameter. Due to mass and volume constraints of launch vehicles, these mirrors could be segmented mirrors, light weight, more flexible. Meeting requirements for surface accuracy and alignment for these mirrors is very challenging. Development of space telescopes, such as Hubble Space Telescope and James Webb Telescope, has been very challenging in terms of cost, schedule, and performance. Considering the past experience of major cost overruns, schedule delays and performance problems in orbit, there is great concern in starting a new program for space telescopes with large apertures. Application of active optics on future spacecraft has the potential to reduce cost and schedule, and higher confidence in meeting on-orbit optical performance.

*Email: agrawal@nps.edu

Micro- and Nanotechnology Sensors, Systems, and Applications VI, edited by Thomas George,
M. Saif Islam, Achyut K. Dutta, Proc. of SPIE Vol. 9083, 90830N · © 2014 SPIE
CCC code: 0277-786X/14/$18 · doi: 10.1117/12.2050014

2.1 Segmented Mirror Telescope [1]. [2], [3]

The Naval Postgraduate School (NPS) received a 3 meter diameter Segmented Mirror Telescope (SMT) that uses Active Hybrid Mirror (AHM) technology for the active control of segmented mirrors. Actuated hybrid mirrors are hybrid structures. They integrate a precision Nanolaminate foil facesheet with a Silicon Carbide (SiC) substrate equipped with embedded electroactive ceramic actuators. Nanolaminate foils consist of many layers; a carbon separation layer to remove it from the mandrel, a layer that forms the optical surface of the mirror, alternating layers of a crystalline metallic, and an amorphous layer. Nanolaminates are deposited on super polished glass or metal mandrels, which are figured to closely match the reverse of the desired optical figure. The SiC substrate is designed for lightweight, toughness, and smooth actuation. Embedded in the substrates are electrostrictive ceramic actuators that are oriented parallel to the surface of the mirror. These actuators are very low hysteresis and low creep devices. They provide both local and global influence for shape control.

Figure 1. Segmented Mirror Telescope and Optical Test Setup

SMT as shown in Figure 1 consists of six segments. Each segment has 156 face sheet actuators (FSA) for surface control and 3 fine and six coarse actuators for segment alignment. A Shack-Hartman wave front sensor is used for surface control and a phase diversity sensor is used as sensor for segment alignment. A Fast Steering Mirror (FSM) is used for jitter control.

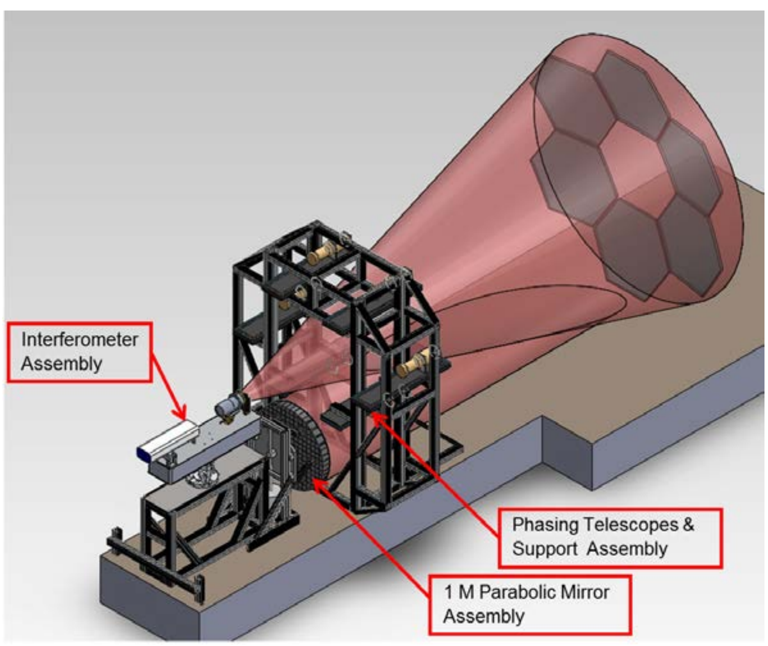

Figure 2. Conceptual view of SMT Testbed

Conceptual view of the testbed is shown in Fig, 2. It consists of three experiments. First, an interferometer and null corrector for center of curvature test. Second, phasing telescopes used to phase the edges of adjacent segments. Third, a 1 meter parabolic mirror for generating 1 meter collimated laser beam for testing SMT sensor suite.

2.2 Center of Curvature Test

The procedure for center of curvature test is as follows. The laser interferometer and the null corrector are mounted to make the primary mirror look like a spherical mirror at the primary mirror center-of-curvature. The laser beam from the interferometer passes through the null corrector at the center-of-curvature and out to the primary mirror segments. The reflected beam passes back through the null corrector and then into the interferometer. The interferometer measures the wavefront error and can be used to drive the face sheet actuators to minimize the aberrations present in the segments.

The procedure for generating an influence function is as follows. Xinetics developed the segments and provided initial FSA voltage values for surface correction. With Xinetics voltages applied to FSAs the interferometer is aligned to the segments using a hexapod or the SMT coarse control actuators (CCAs). A voltage of 25V and a 75V is applied to each FSA and an interferogram is taken at each voltage. This results in 312 interferograms for each segment. Each image is the average of 5 interferometer measurements and the total process takes approximately 1 hour. Subtracting low and high measurements from each actuator to produces 156 influence functions. Using an optimization algorithm voltage changes to the FSAs are determined to improve segment surface figure from the Xinetics baseline voltages. The segment surface is re-measured and compared to the initial surface. The process is repeated until there is no further improvement on wave front error. Influence functions are shown in Fig. 3 and the improved segments surface is shown in Fig. 4.

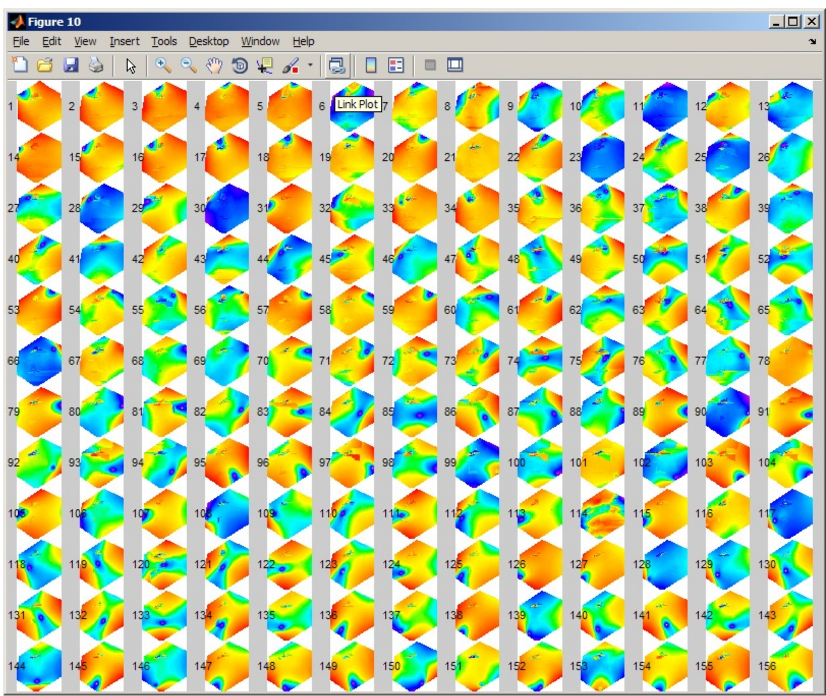

.

Figure 3. Images of 156 influence functions

Figure 4 shows 972 nm RMS wave front error by applying Xinetics voltages and shows 348 nm RMS error after applying optimized voltages to the actuator during initial iterations.

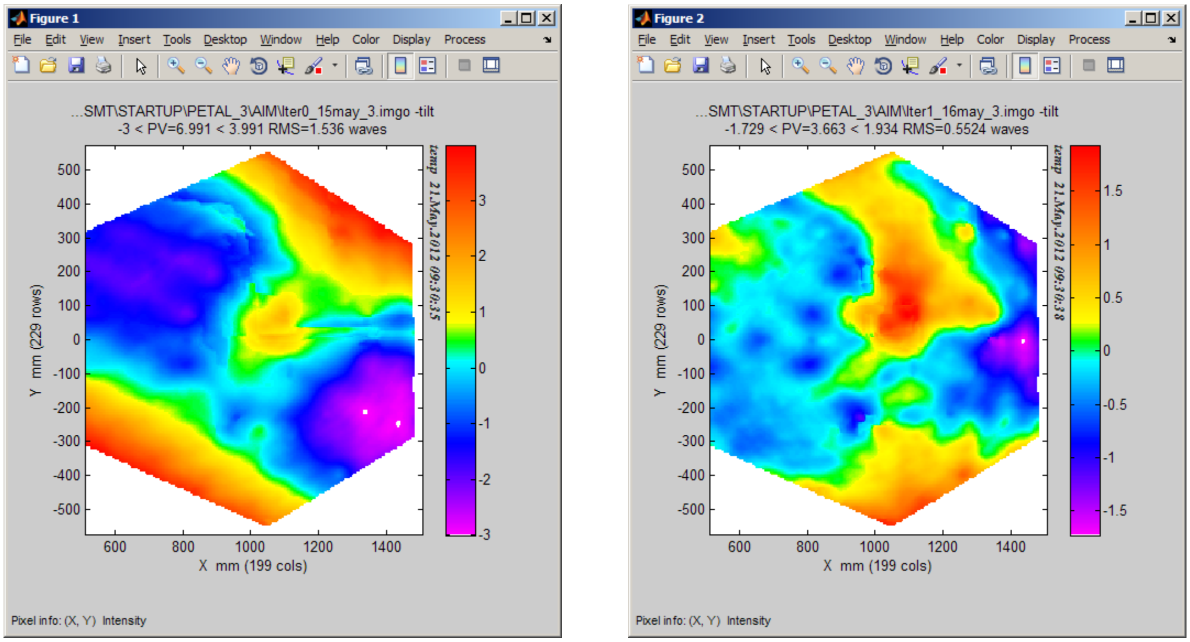

Figure 4. Initial Xinetics FSA Voltages applied 972 nm RMS (left) and Optimized FSA Voltages applied Resulting in 348 nm RMS error (right)

2.3 Tuned Mass Dampers [4]

Structural modes of the SMT are being excited in a laboratory environment. The wave front error due to this excitation is more than the wavelength. In order to use phase diversity sensor for segment phasing, wave front error should be less than quarter wavelength. Experimentally derived modes are given in Figure 5 and their influence on wavefront is shown in Figure 6.

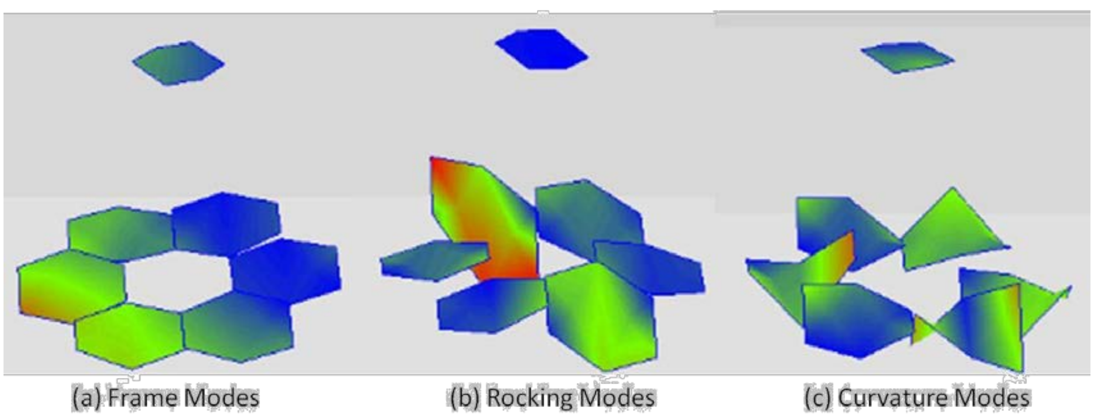

Figure 5. SMT Structural Modes

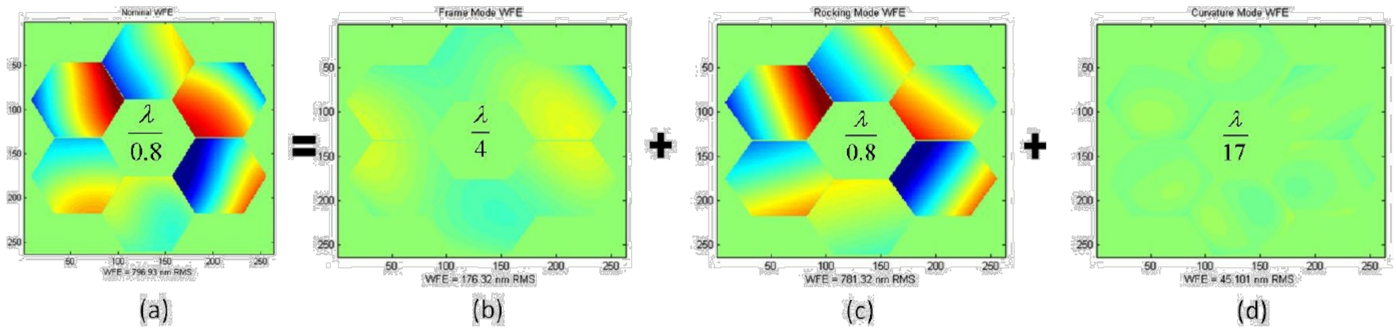

Figure 6. Influence on Wavefront Error

Rocking mode was the main contributor of wavefront error. Therefore magnetic tuned mass dampers (TMDs) were used to reduce vibration for the rocking modes. TMDs were successful in improving the WFE by a factor of five and reduce disturbance by 80% within the dynamic range of the on-board sensors as shown in Figure 7.

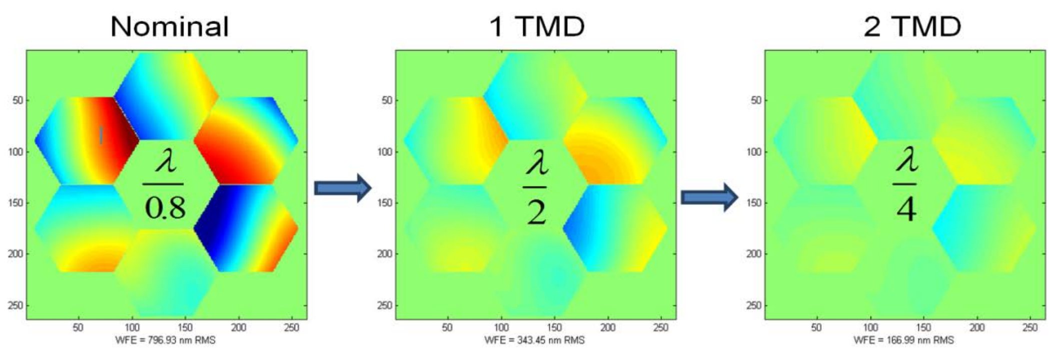

Figure 7. Wavefront Error Correction Using TMDs

2.4 Addition of Deformable Mirror to SMT Optical Path [5]

The objective is to add a deformable mirror (DM) into the SMT optical path to correct for residual beam aberration not corrected by the primary mirror actuators. This reduces surface performance requirement on the primary mirror, reducing overall cost and schedule for testing. This also provides a robust and self- correcting design. One possible configuration for SMT will be to replace second fold mirror with a DM in the optical path. Shack-Hartmann and phase diversity wavefront sensors can be used as feedback sensors for the deformable mirror. To evaluate this approach, deformable mirror has been added in the optical path for center of curvature test as shown in Figure 8.

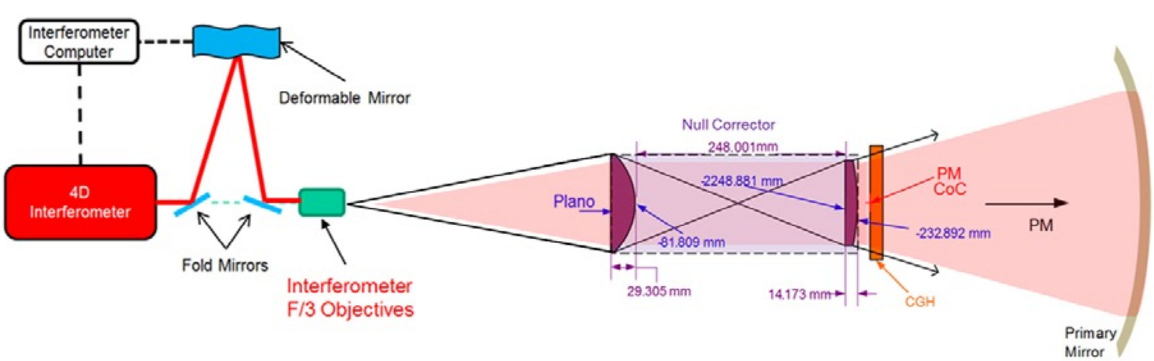

Figure 8. Center of Curvature Experiment with Deformable Mirror Inserted into Optical Path

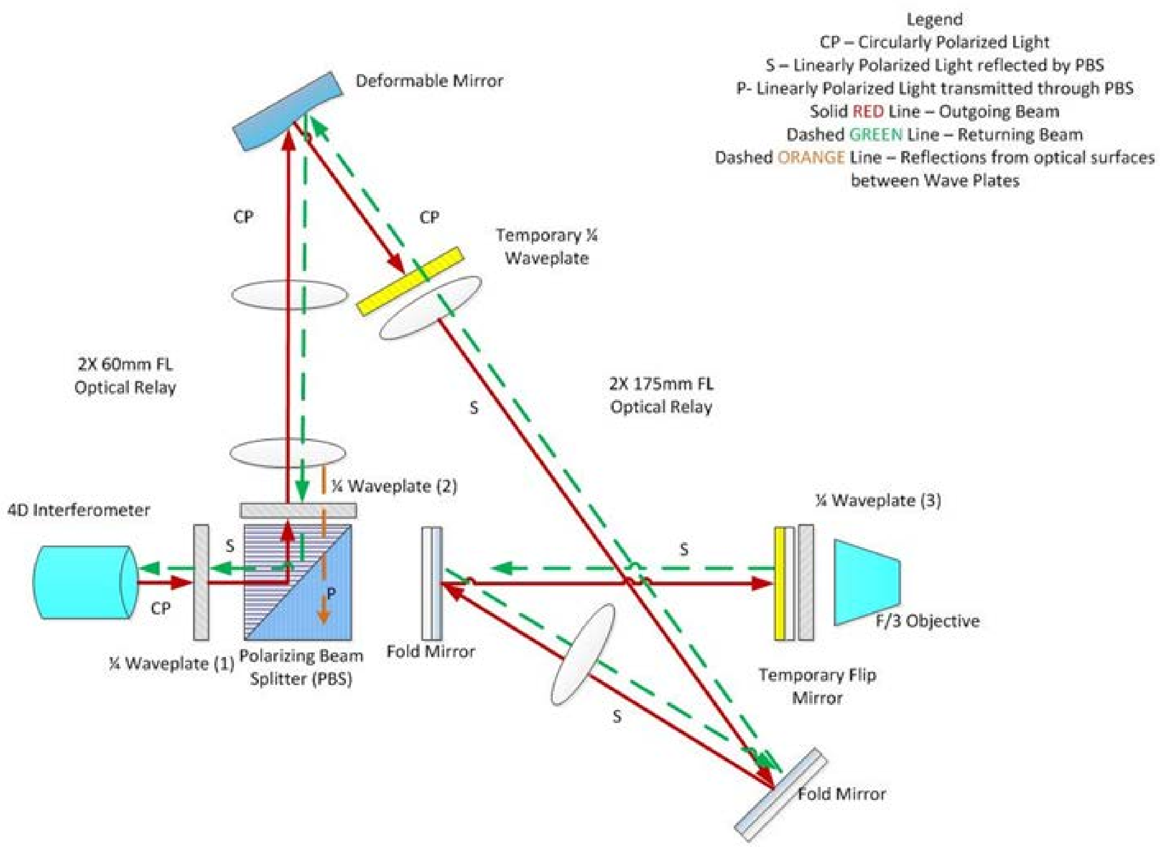

Figure 9. Optical Setup for Deformable Mirror.

The experiment was performed in two steps. First, the primary mirror surface was corrected by using face sheet actuators and bypassing optical path of deformable mirror. Next, the deformable mirror was used to correct the residual wave front error from the primary mirror. The deformable mirror has lower and upper bound for actuator voltages. So constrained optimization techniques were used. The current deformable mirror can reduce RMS wave front error by 55%. The limitations were due to small number of actuators. In future, we plan to use DM with significantly larger number of actuators. In summary, deformable mirrors can be effective to correct surface errors of primary mirrors of imaging satellites.

3. HIGH ENERGY LASER BEAM CONTROL

Beam control is a critical element for High Energy Laser (HEL) systems with a stable line-of-sight requirement. Various disturbances such as mechanical vibration, static and dynamic loading, and thermal and acoustic effects cause optical jitter and severely degrade the performance of optical systems. In addition, atmospheric turbulence causes aberration in the wavefront of a laser beam, which poses significant challenges in beam control. Beam control addresses rejection of these time-varying disturbances by real-time active control with various sensors and actuators.

3.1 Acquisition, Tracking, and Pointing and Optical Jitter Control [6]

Acquisition, Tracking, and Pointing Using Low Power Beam Control Testbed

Acquisition, Tracking, and Pointing (ATP) and optical jitter control are a pre-requisite for high order beam corrections using Adaptive Optics (AO). The low power testbed shown in Figure 10 is an integrated beam control testbed for ATP and optical jitter control.

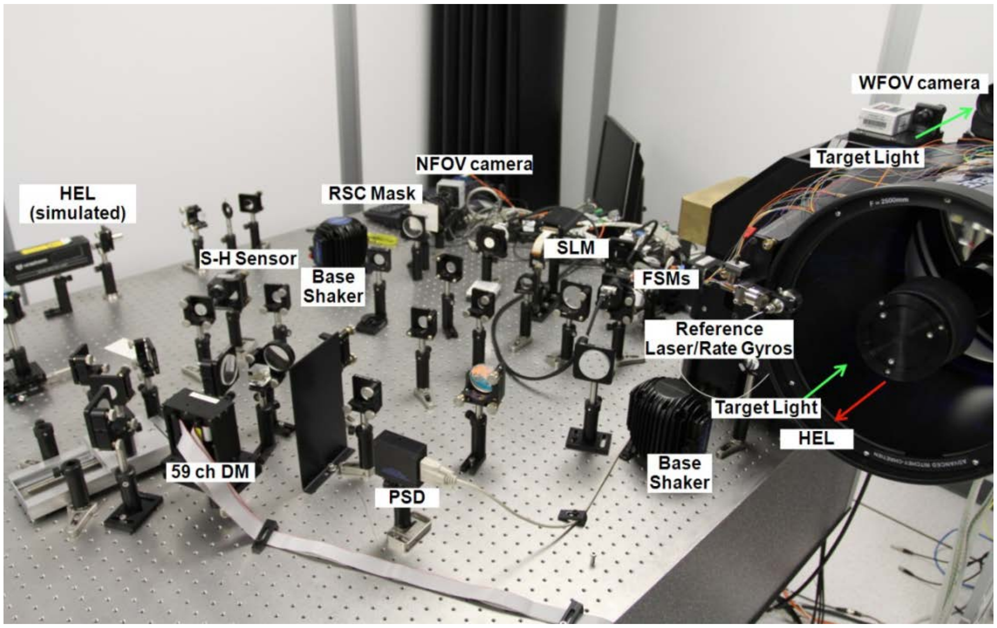

Figure 10. Low power beam control testbed

The testbed incorporates major beam control components including a 10 inch AZ-EL gimbaled telescope, Wild Field of View (WFOV) and Narrow Field of View (NFOV) trackers, fast steering mirrors, a deformable mirror, a wavefront sensor, a strap-down inertial reference laser, and a spatial light modulator for turbulence simulation. The schematic of the testbed is shown in Figure 11. Figure 12 depicts the operation of the testbed when the laser is engaged to the target through the beam path extension mirror.

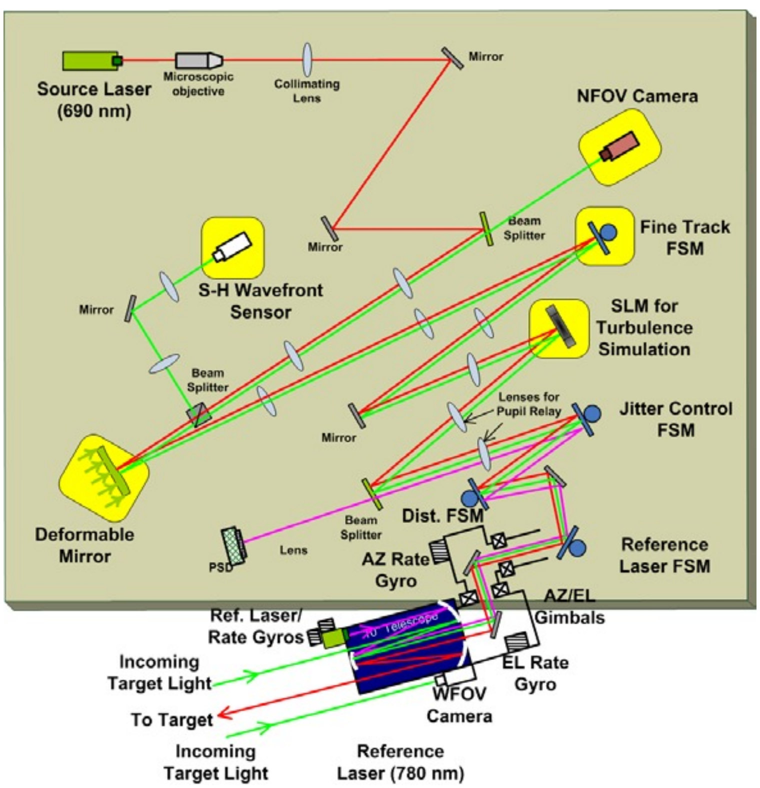

Figure 11. Schematics of the Low Power Beam Control Testbed

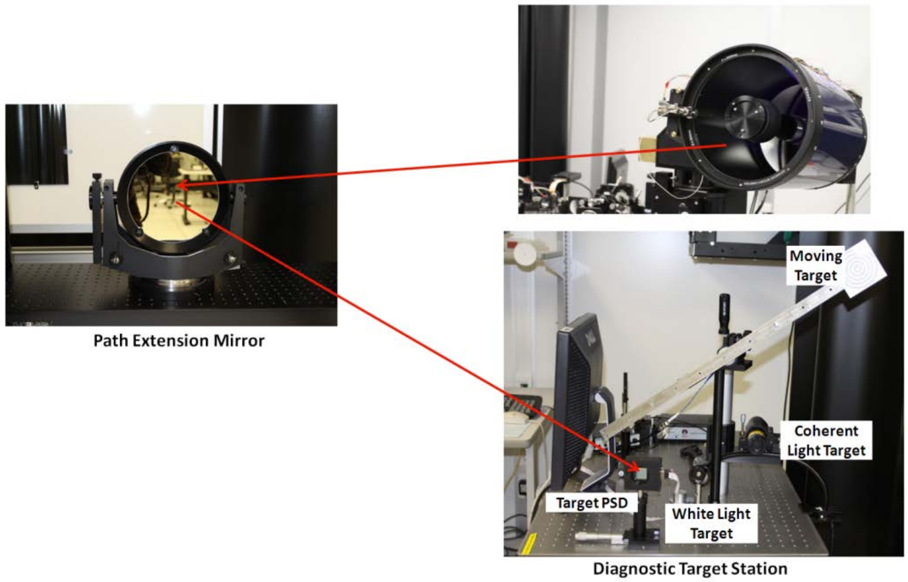

Figure 12. Schematics of the Low Power Beam Control Testbed

Adaptive Filter Control for Fine Tracking and Beam jitter Control

The dynamically changing nature of disturbances makes adaptive filters desirable to replace or augment conventional fixed-parameter control feedback loops. The function of the adaptive filter is to modify an incoming reference signal that is correlated with the disturbance to cancel a disturbance applied to the system. Modification of the reference signal is performed by the Finite Impulse Response (FIR) filter of the form;

$$y(n) = \sum_{i=0}^{L} w_i(n)x(n-i) = \boldsymbol{w}^T(n)\boldsymbol{x}(n) \tag{1}$$

Where $\boldsymbol{w}(n)$ is the filter weight vector of length L whose i^{th} component is $w_i(n)$, $\boldsymbol{x}(n)$ is the vector of delayed inputs, $\boldsymbol{x}(n-i)$, and $\boldsymbol{y}(n)$ is the filter output. Figure 13 shows the FIR filter structure where the filter weights are adaptively determined

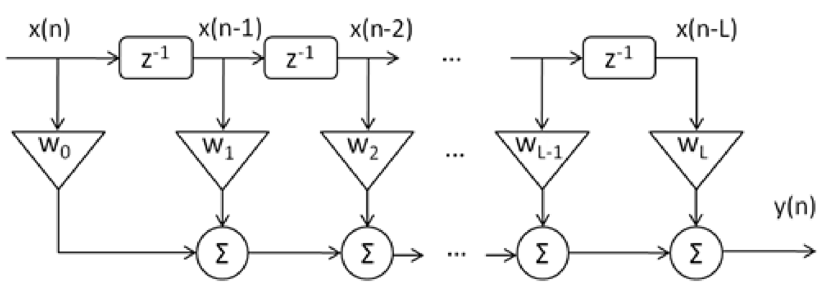

Figure 13. Transverse FIR filter structure

Least Mean Square (LMS) and Recursive Least Square (RLS) are two common algorithms widely used to update the filter weights. In the LMS algorithm, the cost function $\zeta(n)$ is the expectation of $\boldsymbol{e}(n)^2$called Mean Square Error (MSE) denoted by $E\{\mathbf{e}(n)^2\}$. When the statistics of the disturbance and the reference signal are available, the weights that minimize $E\{\mathbf{e}(n)^2\}$ can be computed. In practice, however, such a priori information is often unavailable. In LMS algorithm, the MSE is approximated by the instantaneous squared error and iterative steepest-gradient descent method is used to update the weights in the direction toward lowest error. The difference equation for updating weights can be expressed as

$$\boldsymbol{w}(n+1) = \boldsymbol{w}(n) - \frac{\mu}{2}\frac{\partial J[n]}{\partial \boldsymbol{w}(n)} = \mathbf{w}(n) + \mu e(n)\mathbf{x}(n) \tag{2}$$

where μ is the convergence coefficient that controls the speed of the convergence to steady-state weight values.

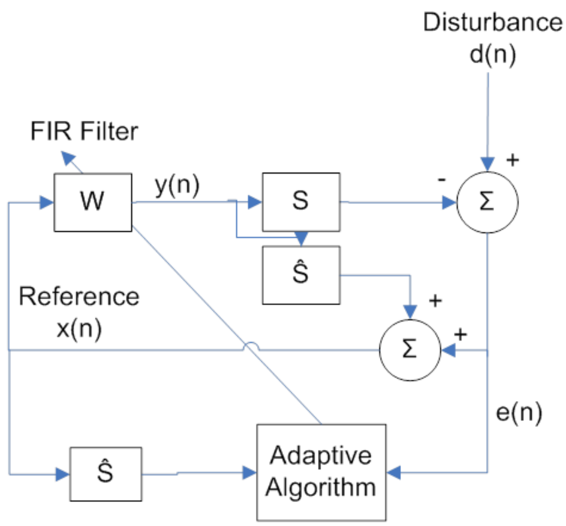

Figure 14: Filtered-X feedback adaptive filter control diagram with internally generated reference signal

The practical challenge with the adaptive filters is that they require a reference signal that is correlated with the disturbance. In case it is not possible or very expensive to obtain this disturbance correlated signal, the estimated disturbance can be generated from the observed error to be used as a reference. In addition, the filtered signal passes through a physical actuator (secondary plant) before it counteracts with the disturbances. This secondary plant effects are also need to be considered. Figure 14 shows the feedback adaptive filter control design including the secondary plant S, estimate of the secondary plant $\hat{S}$, and internally generated reference signal x(n). The adaptive filter can address periodic components of the disturbance well and its adaptive nature allows the controller to track the frequency change of the periodic components. To overcome the limitation of the feedback adaptive filter for broadband disturbance, a PI controller can be combined with an adaptive filter as shown in Figure 15, where G is the open loop transfer function of the secondary plant including PI control design.

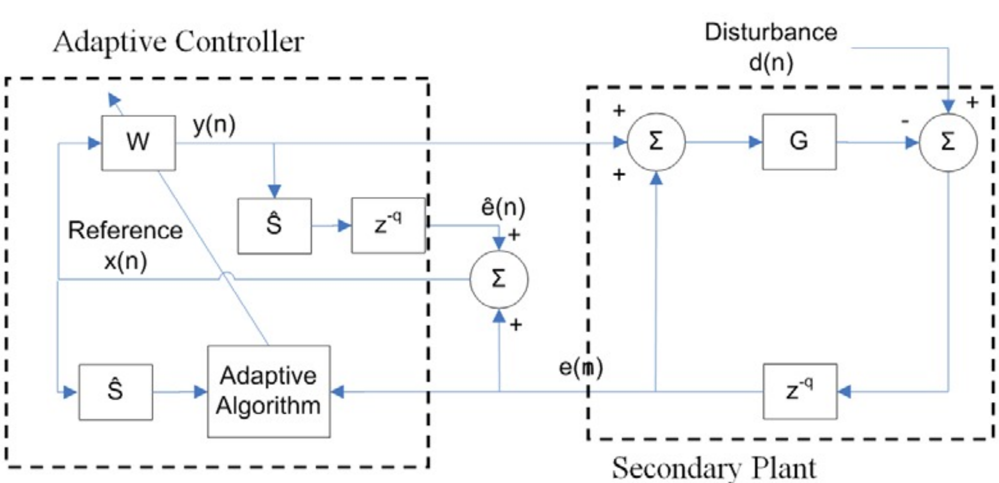

Figure 15. Adaptive filter control augmenting a PI controller

Experiments are performed using the low power beam control testbed to verify and evaluate the performance of adaptive filter designs for fine tracking and optical jitter control [7]. Figure 16 and Figure 17 shows a Narrow Field-of-View (NFOV) video tracking control results with and without adaptive filter control integrated into the classical control design.

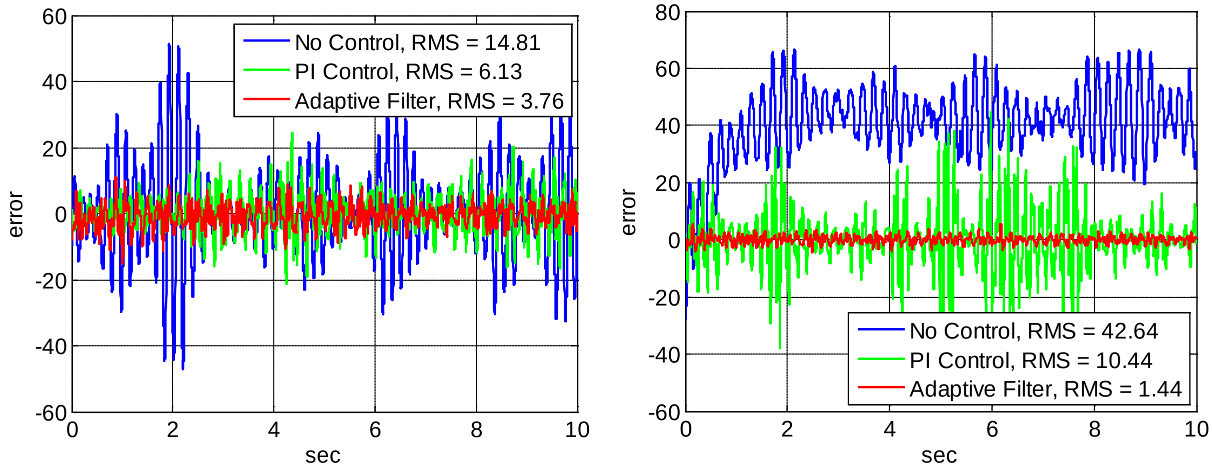

Figure 16. Time Domain Error (Left: X-axis, Right: Y-axis)

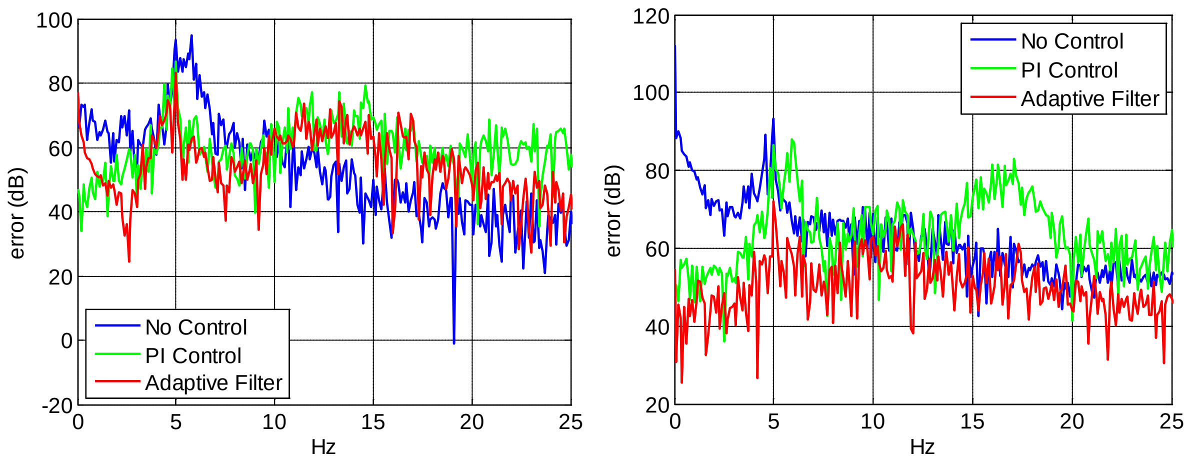

Figure 17. Frequency Domain Error (Left: X-axis, Right: Y-axis)

3.2 Adaptive Optics

Adaptive optics is a technology used to improve the performance of optical systems by compensating the effect of wavefront distortions due to the atmospheric turbulence. The conventional application of AO technology has proven to be successful in correcting weak atmospheric turbulence, essentially near field turbulence. The laser beam aberrations in this regime are primarily in the phase. Such turbulence is experienced by astronomical telescopes usually built on the top of mountains. For low altitude over near horizontal paths, the turbulence becomes strong and possibly non-homogenous. Deep turbulence contains far-field scintillation that creates intensity peaks and nulls due to the propagating laser beam interfering with itself. This poses significant challenges in adaptive optics.

Simulation of Atmospheric Turbulence

In order to test an adaptive optic system and control methods being developed at the AOCoE, a Liquid Crystal (LC) Spatial Light Modulator (SLM) is being used to generate atmospheric turbulence in the laboratory.

Figure 18: Liquid Crystal Spatial Light Modulator by Boulder Nonlinear Systems

Using an LC SLM in combination with wave optic simulation software that generates atmospheric turbulence can provide the desired flexibility to reproduce the prescribed atmospheric conditions in the laboratory. To generate both phase and amplitude, the Boulder Nonlinear Systems (BNS) LC SLM shown in Figure 18 is used. The LC SLM has a 512x512 pixel format with 15x15 μm/pixel pitch, and can operate at a maximum sampling rate of 1 kHz. Wave-optic propagation software was used for programming varying turbulence strength into the BNS LC SLM for characterization of deep turbulence and reproducing the turbulence scenario in the laboratory. The LC SLM also allows the use of field measured data instead of computer simulation for better representation of deep turbulence environment in the future.

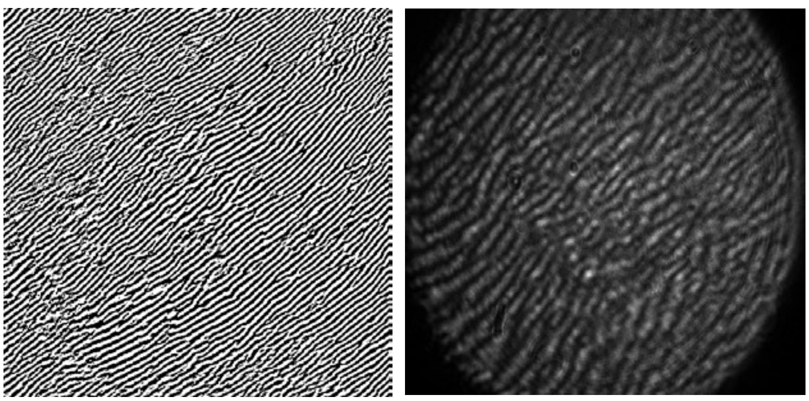

(a) Software simulation (b) Laboratory generated using SLM

Figure 19. Phase comparison between software simulation and laboratory generated (Cn^2= 9e-14, Rytov=3.923)

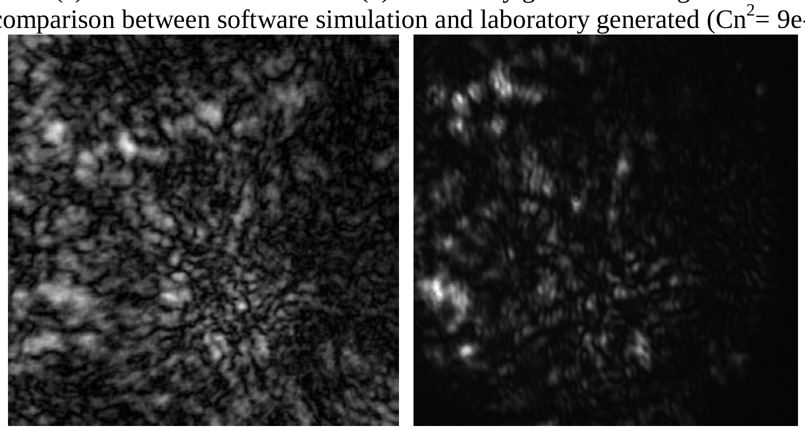

(a) Software simulation (b) Laboratory generated using SLM

Figure 20. Amplitude comparison between software simulation and laboratory generated (Cn^2= 9e-14, Rytov=3.923)

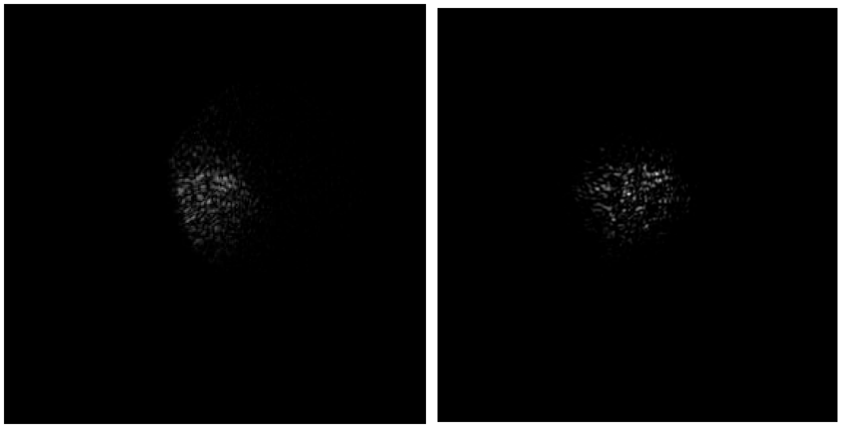

(a) Software simulation (b) Laboratory generated using SLM

Figure 21. PSF comparison between software simulation and laboratory generated (Cn^2= 9e-14, Rytov=3.923)

Figures 19-21 show the comparison of WaveProp simulation results and laboratory experimental results for amplitude, phase, and point spread function of a beam from a point source target.

Adaptive Optics Testbed

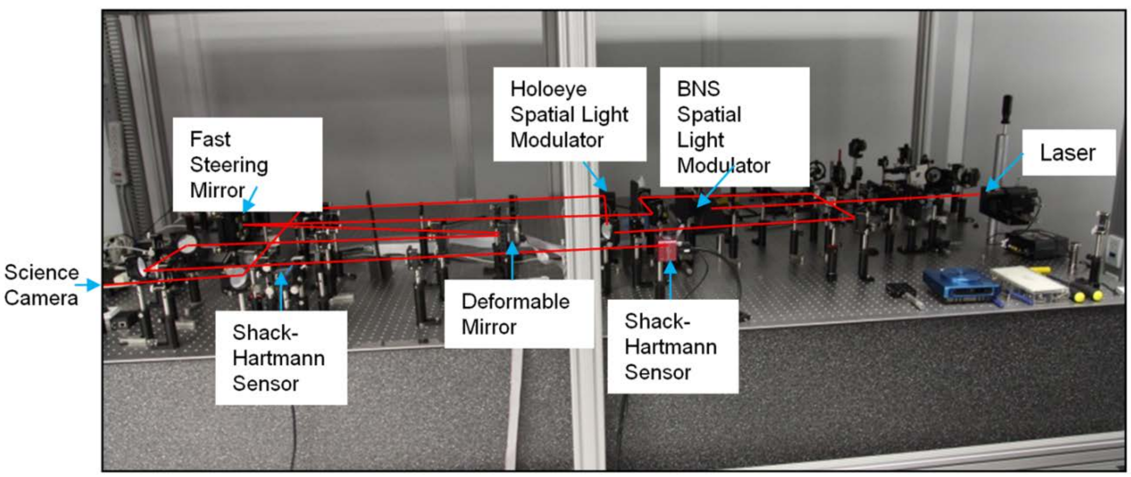

Figure 22. Adaptive Optics Testbed

In order to study adaptive optics mitigation and demonstrate advanced AO compensation techniques, NPS has developed an AO testbed as shown in Figure 22. The testbed consists of a 632nm laser acting as an AO beacon, translucent Spatial Light Modulator (SLM) (Holoeye Corporation, 800x600, 60 Hz), Shack Hartmann Wavefront Sensors (SHWS) (127 microlens-array), a deformable mirror (37 channel OKO MMDM), and science cameras for pupil and amplitude spread function imaging. The atmospheric turbulence was simulated by modulating the phase using the SLM and real-time adaptive optics compensation was performed using a Matlab/xPC real-time operating system. Using this AO testbed, NPS performs various experiments by applying advanced AO control methods.

Advanced Adaptive Optics Control

In order to cope with high spatial and temporal resolution required for adaptive optics compensation in the deep turbulence regime, advanced adaptive optics control techniques are investigated to provide greater flexibility in control design.

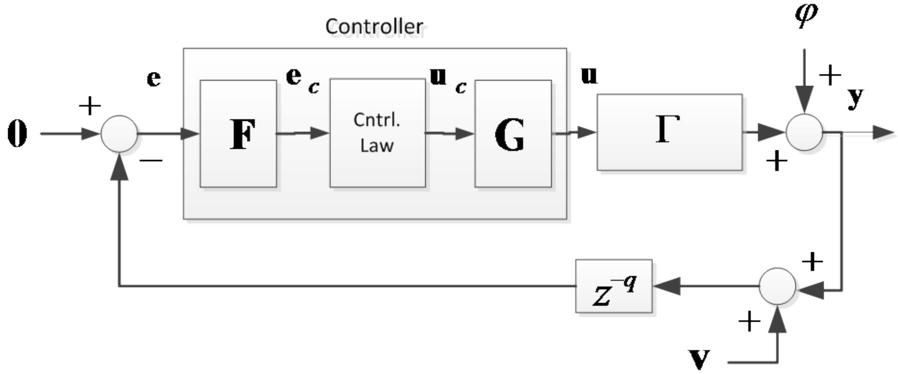

Figure 23. Block diagram of a modal reduction control system

Figure 23 shows the block diagram of the modal reduction control system. The plant is modelled as an influence matrix Γ. An arbitrary choice of matrix, **F**, was used in Figure 23, with an additional matrix **G** to provide the decoupled relationship from $\mathbf{e}_c(k)$ to $\mathbf{u}_c(k)$. For a decoupled path, **G** has to be selected as $\mathbf{G} = (\mathbf{F}\Gamma)^{\dagger}$ such that

$$\mathbf{e}_c(k) = -\mathbf{F}\Gamma\mathbf{G}\,\mathbf{u}_c(k) = -\mathbf{F}\Gamma\left(\mathbf{F}\Gamma\right)^{\dagger}\mathbf{u}_c(k) = -\Sigma\mathbf{u}_c(k) \tag{3}$$

where, Σ is a diagonal matrix. This is the basis of the modal control method which allows us to scale the dimension of the controller design space by selecting a proper modal basis. Modal reduction by retaining only significant modes through this modal control scheme can provide computationally efficient and robust control design. The matrix **F** projects the wavefront sensor information using a modal basis represented by the columns of the matrix **F**. Therefore, one can have freedom to select an appropriate scalable modal basis to reconstruct the wavefront error information used by the controller. Table 1 shows the different modal basis considered for the control design.

Table 1. DIFFERENT TYPE OF MODAL BASIS

Pseudo Inverse	Singular Value Decomposition (SVD)	Zernike	Orthogonalized Zernike
• Pseudo-inverse of the poke matrix. • Modes are equivalent of column vectors of the poke matrix with some scaling.	• SVD of the poke matrix. • Orthogonality guaranteed. • Modes are ordered for the effectiveness of the DM.	• A series of polynomials orthonormal in a unit circle. • Orthogonal for a circular aperture. • Traditionally used in optics.	• Zernike modes are orthogonalized as finite dimension vectors preserving the spatial characteristics. • Higher order modes depart from the corresponding Zernike modes.

Figure 24 shows the experimental results of modal control method using the adaptive optics testbed. Figure 25 shows the time mean average of the sensor error using a modal control with PI controller. The results suggested that good adaptive performance can be achieved even with the reduced number of modes, which is directly related to the reduced number of control channels and computation required.

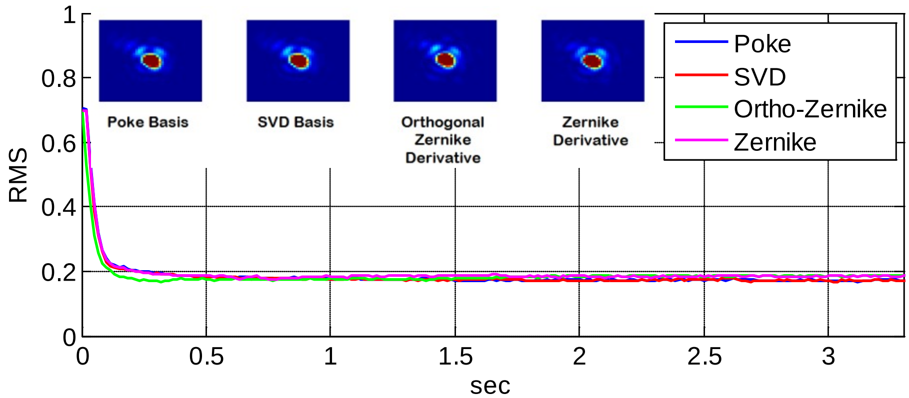

Figure 24. RMS of the error vector components with different modal basis

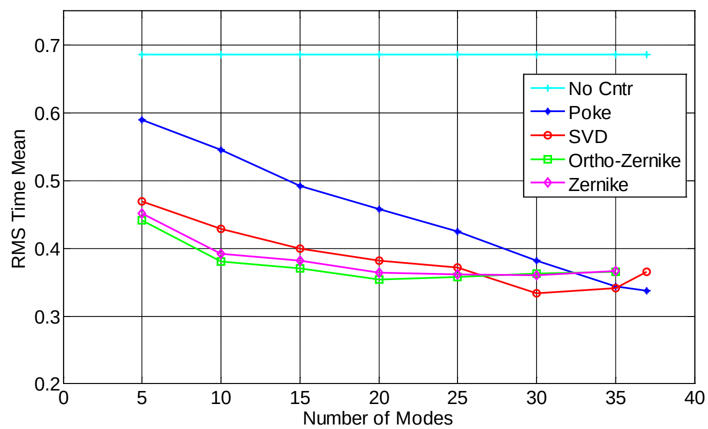

Figure 25. Time mean of the sensor error RMS by Modal Control with PI controller

Adaptive filter control used for fine beam steering and pointing can be also applied for adaptive control. Figure 26 shows the block diagram of the adaptive optics control with augmented adaptive filter control. The experimental results shown in Figure 27 suggests that better AO performance is achieved when the augmented adaptive filter control and modal control design is applied to the adaptive optics testbed, compared to conventional PI control design.

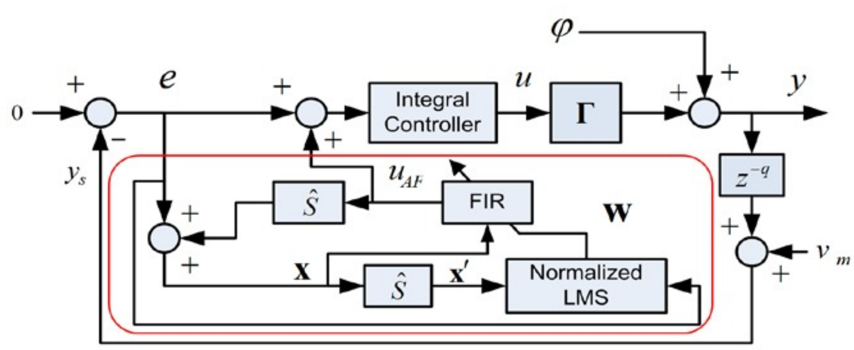

Figure 26. AO Control system diagram with augmented adaptive filter control

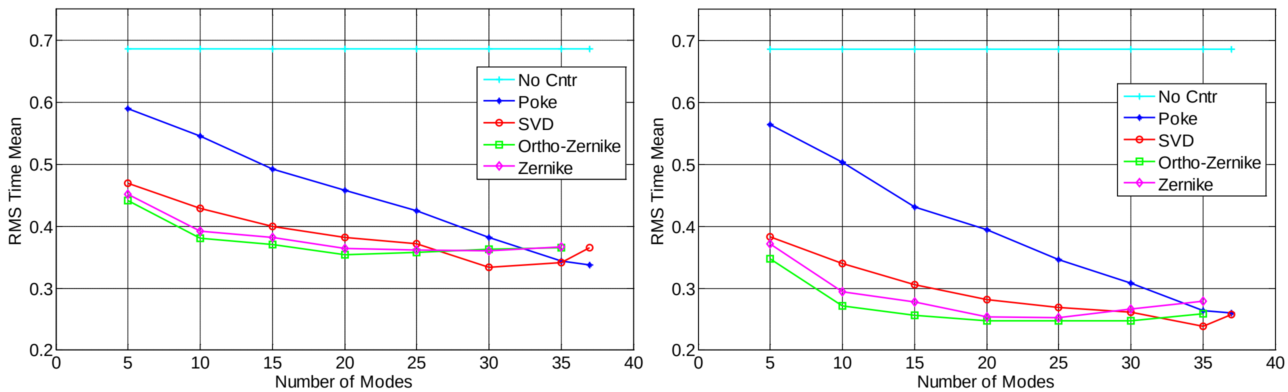

Figure 27. Time mean average of the sensor error - PI control (left) and augmented adaptive filter control (right) using different modal basis

4. SUMMARY AND CONCLUSIONS

In summary, adaptive optics is a complex and multidisciplinary research area and has applications in several future systems for national security. At the Adaptive Optics Center of Excellence for National Security, major progress has been made in research and development of segmented mirror telescope and high energy laser beam control test beds. Major current focus areas are to validate and develop improved technologies to reduce risk, cost, and schedule for future DoD programs, such as imaging satellites, HEL beam control, and laser communications; collaborate with universities, space industry, national labs, and DoD program offices; and educate military and DoD civilians in this multidisciplinary field of optics, structures, and control and give hands-on experience on these test beds.

5. ACKNOWLEDGEMENTS

The author would like to sincerely acknowledge the contributions of the members of Adaptive Optics Center of Excellence for National Security at NPS. The contributors include Dr. Ty Martinez, Dr. Jae Jun Kim, Dr. Lewis DeSandre, Dr. John Bagnasco, and Dr. Bautista Fernandez.

REFERENCES

[1] Hickey, G., Ealey, M., and Redding, D., "Actuated Hybrid Mirrors for Space Telescopes", SPIE Space Telescopes and Instrumentation, Vol. 7731, 773120-1, 2010.

[2] Agrawal, B. and Kim, J. J., "Surface Control of Actuated Hybrid Space Mirrors",Proceeding of 61th International Astronautical Congress, 27 Sepember-1 October, 2010, Prague, Czech Republic, IAC-10.C2.5.8.

[3] Kim, J. J., Burtz, D. and Agrawal, B., "Wavefront Correction of Optical Beam for Large Space Mirrors Using Robust Control Techniques", Acta Astronautica, Volume 68, Issues 1-2, pp. 141-148, January-February 2011.

[4] Yingling, A. J. Yingling and Agrawal, B. "Applications of Tuned Mass Dampers to Improve Performance of Large space Mirrors", Proceeding of 63rd International Astronautical Congress, September 2012, Naples, Italy, IAC-12.C2.5.4x13800.

[5] *Zhu, L., Sun, P.C., Bartsch, D. U., Freeman, W. R., & Fainman, Y., "Adaptive Control of a* Micromachined Continuous-Membrane Deformable Mirror for Aberration Compensation", Applied Optics, 38, 168-*176., 1999.*

[6] Allen, M., Kim, J. J. and Agrawal, B., "Control of a Deformable Mirror Subject to Structural Disturbance", SPIE Defense and Security Symposium, Orland, FL, March 2008.

[7] J. J. Kim, M. Nagashima, and B.N. Agrawal, "Optical Beam Jitter Control for NPS HEL Beam Control Testbed," 14th Annual Directed Energy Symposium, 14-18 November 2011, San Diego 11-Symp-080.